ISSN 1028-334X, Doklady Earth Sciences, 2023, Vol. 512, Part 1, pp. 793–800. © The Author(s), 2023. This article is an open access publication, corrected publication 2023.
ISSN 1028-334X, Doklady Earth Sciences, 2023. © The Author(s), 2023. This article is an open access publication, corrected publication 2023.
Russian Text © The Author(s), 2023, published in Doklady Rossiiskoi Akademii Nauk. Nauki o Zemle, 2023, Vol. 512, No. 1, pp. 29–38.

GEOLOGY OF ORE DEPOSITS

Long Evolution of a Magmatic–Ore System of the Muruntau Gold Deposit, Western Uzbekistan, Tien Shan: Evidence from the LA–ICP–MS U–Pb Isotopic Age of Zircon from Granitoids of the Sardara (Sarykty) Pluton

S. G. Soloviev[a,*], S. G. Kryazhev[b], D. V. Semenova[c], Yu. A. Kalinin[c], and Academician N. S. Bortnikov[a]

Received February 2, 2022; revised May 5, 2023; accepted May 12, 2023

Abstract—The LA–ICP–MS U–Pb age was determined for the first time for zircon from granodiorites–granites of the Sardara (Sarykty) intrusive in area of the giant Muruntau gold deposit in Western Tien Shan (Uzbekistan). Three crystal groups were identified in a combined sample: their concordant U–Pb age is 322.0 ± 3.7 (four grains), 301.6 ± 2.1 (11 grains), and 289.5 ± 4.9 Ma (two grains) (MSWD = 3.1, 0.17, and 0.98, respectively). The dispersion of the isotopic age can be explained using a model of a successive crystallization of different zircon generations in magmatic chambers at various depths and their further entrapment upon differentiation/crystallization of new magma portions. The similarity of two (youngest) age intervals with concordant U–Pb ages previously published for zircons of granitoid rocks directly at the Muruntau deposit is noteworthy. The latter ages could thus represent dike branching at the corresponding stages of evolution (progressive differentiation) of deeper sources of granitoid magma, the larger intrusions of which include Sardara (Sarykty) and other plutons exposed at some distance from the deposit. The older U–Pb isotopic ages of zircons from granitoids of the Sardara (Sarykty) pluton (~322 and 302 Ma) generally correspond to the subduction stage, whereas the youngest zircons (~289.5 Ma) correspond to the postcollision stage of the region. The origination and initial evolution of the magmatic sources in area of the Muruntau deposit could thus occur under subduction conditions; however, the final differentiation and crystallization of granitoid magma has finished at the postcollision stage.

Keywords: U–Pb isotopic studies, zircon, granitoids, Muruntau gold deposit, Western Tien Shan, Uzbekistan

DOI: 10.1134/S1028334X23601104

INTRODUCTION

Igneous rocks in the area of the Muruntau gold deposit had long been and remain in the focus of study of the genesis and evolution of the magmatic-hydrothermal system of this largest ore object, the reserves and resources of which exceed 6000 t Au [1–3]. At the same time, the known isotopic ages of rocks are few in number and contradictory, although these determinations are of primary importance for the elaboration of the corresponding models of the formation and evolution of this complex multistage deposit.

The Muruntau deposit is located in the western part of the Tien Shan orogenic metallogenic belt, which is extended along the Late Paleozoic active continental margin of the Kazakhstan–Tien Shan Paleocontinent (Fig. 1) [4]. The terranes of the passive margin of the Turkestan Paleoocean, which divided this paleocontinent from the continental blocks of the Tarim and Karakum cratons, were accreted to this margin from the south; the closure of the paleoocean occurred in the Late Carboniferous. In the western part of the southern Tien Shan, these terranes form the Nuratau–Kyzylkum segment, in which the Neoproterozoic metamorphic sequences are overlapped by the Early Paleozoic (Ordovician–Silurian) clastic and flyschoid sediments of the passive margin [5]. The area of the deposit is characterized by Late Carboniferous–Early Permian magmatism including postcollision plutons and dikes of calc-alkaline to subalkaline granitoids, as well as lamprophyres [1–3, 5–7]. This magmatism is responsible for the corresponding prolonged stage of the formation of this deposit, although

[a] *Institute of Geology of Ore Deposits, Petrography, Mineralogy, and Geochemistry, Russian Academy of Sciences, Moscow, 119117 Russia*
[b] *Central Research Institute of Geological Prospecting for Base and Precious Metals (TsNIGRI), Moscow, 117545 Russia*
[c] *Sobolev Institute of Geology and Mineralogy, Siberian Branch, Russian Academy of Sciences, Novosibirsk, 630090 Russia*
**e-mail: serguei07@mail.ru*

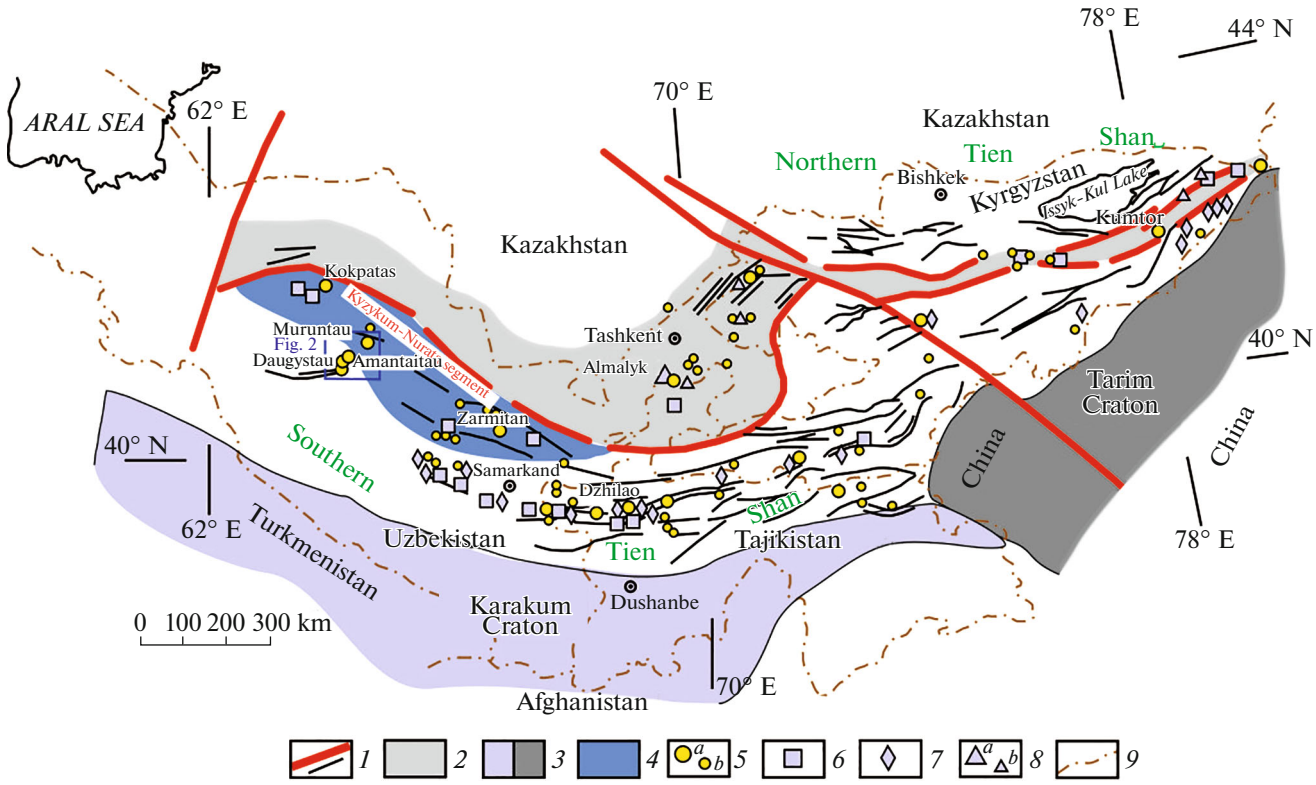

Fig. 1. Scheme of the Late Paleozoic metallogenic belt of Tien Shan. *1*, Faults of different orders; *2*, Late Paleozoic active continental margin (Central Tien Shan); *3*, continental blocks of the basement of the Tarim and Karakum cratons; *4*, terranes of the accretionary wedge thrust on the passive continental margin with a possible cratonic basement; *5* (*a*) main and (*b*) subordinate gold deposits; *6*, W deposits; *7*, Sn deposits; *8*, (*a*) main and (*b*) subordinate porphyry Cu–Mo and Au–Cu deposits; *9*, state boundaries.

this long process is probably not limited solely by magmatism [8].

This deposit contains small stocks of monzodiorites–monzonites (described in some publications as subalkaline diorites–subalkaline quartz diorites of the Myutenbai and other stocks), dikes of felsic rocks (quartz monzonite porphyries and monzogranite porphyries described in some publications as syenite- and granosyenite porphyries), apophyses of leucogranites–alaskites of the larger Murun pluton (exposed by an ultradeep SG-10 borehole at a depth of 4.0–4.2 km), and various dikes of mafic and intermediate rocks including monzogabbro and monzodiorite porphyries and lamprophyres. The monzodiorites–monzonites are typically considered the earliest rocks; however, they predated the Fe–Mg–K (mostly biotite to quartz–feldspar–biotite) metasomatites with disseminated, locally, abundant pyrrhotite, but with a minor Au content. The leucogranites–alaskites of the Murun pluton intrude these metasomatites and contain their xenoliths. The dikes of quartz monzonite porphyries and monzogranite porphyries intrude the early almost barren quartz veins, but predate or accompany gold-bearing metasomatites (with abundant K-feldspar) of the main (early) productive stage. The latter, in turn, predate the late dikes of mafic and intermediate rocks (including lamprophyres), after the intrusion of which the metasomatites with abundant albite and gold-polymetallic mineralization formed.

The area of the Muruntau deposit, at a distance from the ore zones, exposes much larger granitoid plutons (Fig. 2), the rocks of which are often considered part of the igneous association of this deposit with their possible correspondence to some rock varieties (magmatic differentiates), which at the deposit include only small stocks and dikes. The U–Pb ages of zircons are measured for some plutons, in particular, 324–277 Ma (293.5 ± 4.9 Ma, on average) for the Aristantau pluton and 287.7 ± 1.4 Ma for melanocratic granite, 293.3 ± 2.2 for porphyry granite, and 289.3 ± 3.6 Ma for leucocratic granite of the Tamdytau pluton [7]. The Sardara (Sarykty) pluton of granodiorites–granites is exposed ~15 km to the south from the deposit and is the nearest to it. The Rb–Sr isochrone age of the granitoids is 286.2 ± 1.8 Ma [9]. The U–Pb age of zircon from rocks of this pluton, however, was absent, which hampered the corresponding correlation. We filled this gap for the first time.

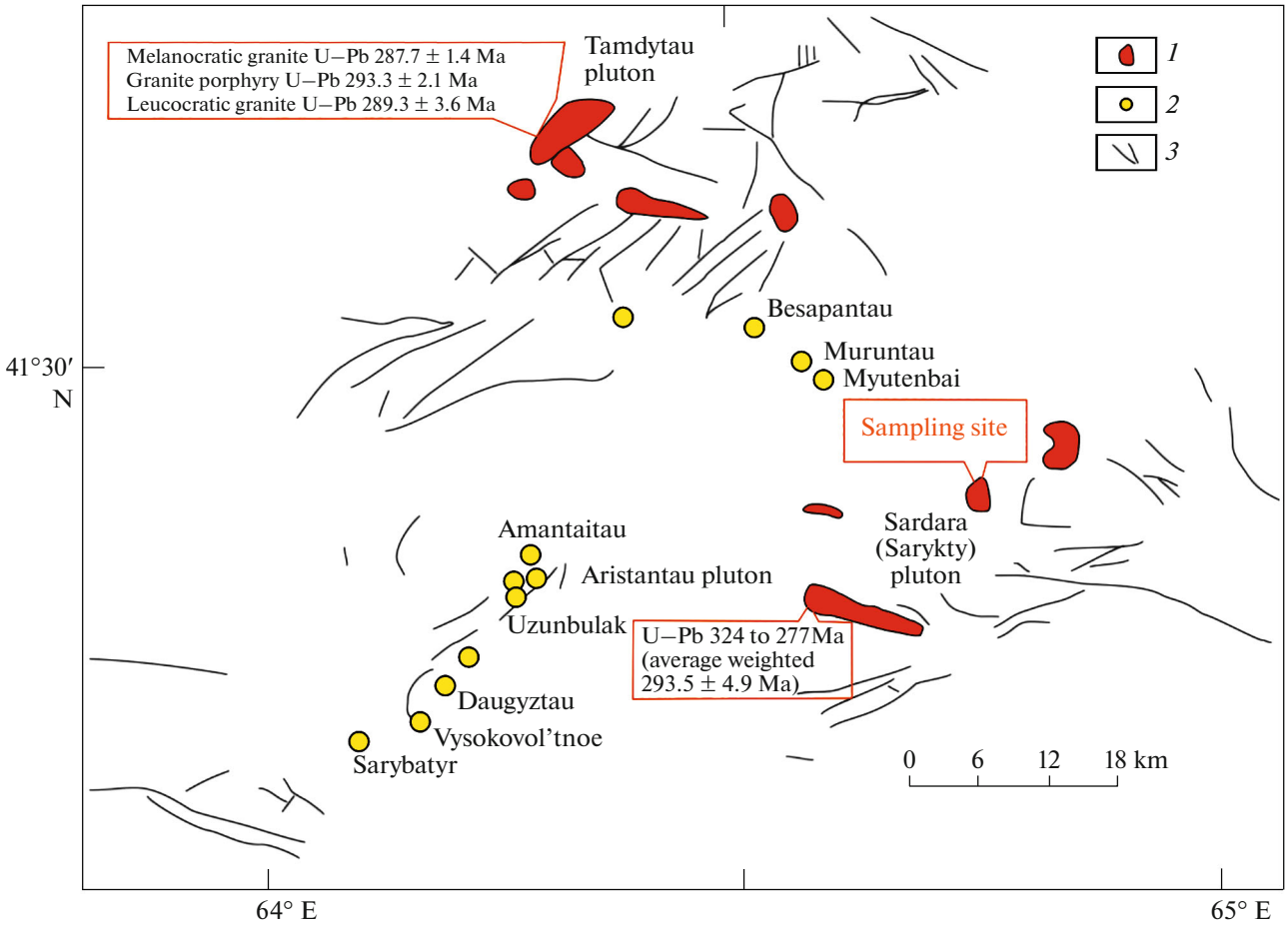

Fig. 2. Location of large intrusives in the area of the Muruntau deposit after [3] (the age of plutons is after [7]). *1*, Intrusives; *2*, gold deposits; *3*, faults.

SAMPLES

For the U–Pb isotopic dating, a sample of granodiorite–granite was taken from the drill core of a prospecting borehole (no. 15) at a depth of 40 m below the erosion surface. The granodiorites–granites of the pluton are the leucocratic medium-grained porphyritic rocks composed of rare amphibole (0–5 vol %), subordinate biotite (5–10 vol %), and dominant plagioclase (30–40 vol %), K-feldspar (30–35 vol %), and quartz (30–35 vol %). Typical large (1–3 cm across) phenocrysts of K-feldspar (orthoclase) comprise 5–10 vol %. The accessory minerals include titanite, apatite, zircon, and the ore mineral. The composition of major oxides and trace elements of rocks is given in Table 1, according to which the granitoids are characterized by higher contents of K, Ba (617 ppm), and Sr (259 ppm), moderately higher contents of Rb (187 ppm), Zr (190 ppm), and Nb (22 ppm), a noticeable enrichment in light rare earth elements, and a clear Eu minimum.

ANALYTICAL METHOD

The U–Pb isotopic studies of zircon crystals were conducted at the Center for Multielemental and Isotopic Studies, Institute of Geology and Mineralogy, Siberian Branch, Russian Academy of Sciences (IGM SB RAS, Novosibirsk, Russia), using an Element XR high-resolution mass spectrometer (Thermo Fisher Scientific) with an Analyte Excite excimer laser ablation system (Teledyne Cetac) equipped with a HelEx II two-chamber cell. The morphology and internal structure of the zircon grains were studied in cathodoluminescent images. The analytical parameters of the mass spectrometer were optimized to achieve a maximum intensity of the ^{208}Pb signal at a minimum $^{248}ThO^{+}/^{232}Th^{+}$ value (<2%) using the NIST SRM612 standard. All measurements were carried out by the ^{202}Hg, ^{204}(Pb + Hg), ^{206}Pb, ^{207}Pb, ^{208}Pb, ^{232}Th, and ^{238}U masses. The analysis was conducted in the E-scan regime. The signals were detected in a counting regime for all isotopes except for ^{238}U and ^{232}Th (triple regime). The diameter of the laser beam was 30 μm, the frequency of pulse repetition was 5 Hz, and the

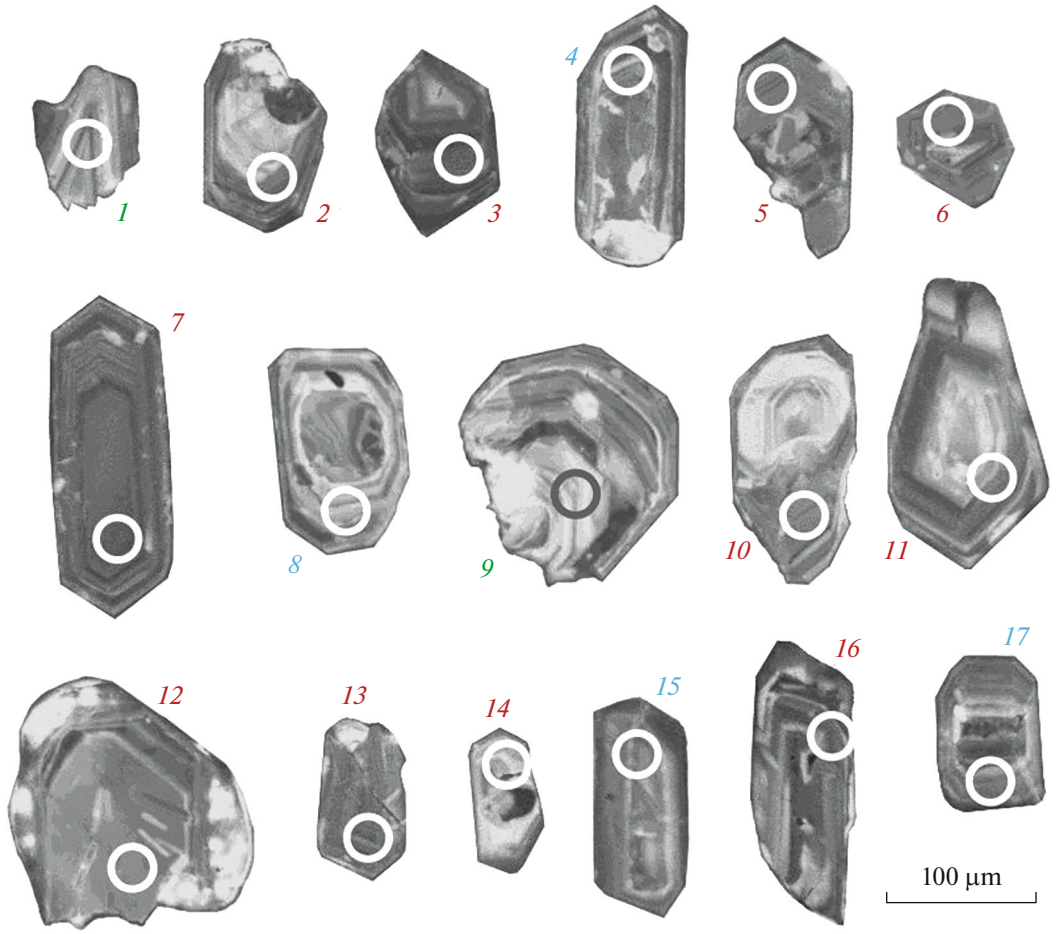

Fig. 3. Cathodoluminescent images of zircon crystals from granodiorites–granites of the Sardara (Sarykty) pluton. Circles indicate areas of isotopic dating; the point numbers correspond to those in Table 2.

energy density of laser radiation was 3 J/cm^2. The mass spectrometric measurements (including calculation of the isotope ratios) were processed in the Glitter program [10]; ^{235}U was calculated from ^{238}U on the basis of a ^{238}U/^{235}U ratio of 137.818 [11]. To account for the elemental and isotopic fractionation, the U–Pb ratios were normalized on the corresponding values of the isotope ratios of the Plesovice standard zircons [12]. The diagrams with concordia were plotted in the Isoplot program [13]. The quality was controlled by the Temora-2 standard zircon [14] with an age of 413 ± 3 Ma (2σ, n = 9).

RESULTS

The zircon crystals in the studied granodiorite–granite sample of the Sardara (Sarykty) pluton are transparent, light pink, well faceted, tabular and elongated prismatic individuals 100–200 μm long with an elongation coefficient of 1.5–2.0 to 3–4 (Fig. 3). In CL images, most crystals exhibit an azoned prismatic core and a fine-zoned rim of various sizes. The U–Pb ages were measured for 17 zircon grains (Table 2, Fig. 3),

Table 1. Content of major oxides and trace elements in a granodiorite–granite sample of the Sardara (Sarykty) pluton

wt %		ppm		ppm		ppm	
SiO_2	69.42	Ba	617.2	Mo	2.43	Pr	7.02
TiO_2	0.46	Sr	259.0	W	3.15	Nd	27.3
Al_2O_3	14.60	Co	8.18	Cs	6.19	Sm	6.83
Fe_2O_3	1.34	Ni	10.1	Hf	5.23	Eu	1.02
FeO	2.86	V	50.6	Ta	2.15	Gd	5.90
MnO	0.05	Cr	28.7	Th	22.6	Tb	0.94
MgO	0.73	Rb	187.0	U	9.30	Dy	5.03
CaO	2.37	Be	3.84	Cu	29.3	Ho	0.93
Na_2O	4.00	Zr	190.3	Zn	30.2	Er	2.54
K_2O	4.07	Nb	22.4	Pb	28.2	Tm	0.40
P_2O_5	0.10	Y	22.6	La	35.4	Yb	2.45
LOI	0.95	Sn	5.10	Ce	54.5	Lu	0.31
Total	100.95						

The content of components was analyzed using the X-ray fluorescent method (major oxides), volumetric method (FeO), and ICP-MS (trace and rare earth elements) in the laboratory of the Central Research Institute of Geological Prospecting for Base and Precious Metals (Moscow, Russia).

Table 2. Results of U–Pb isotopic studies of zircon of granodiorites–granites of the Sardara (Sarykty) pluton

Number of analytical point	Content, ppm		Th/U	Isotope ratios				Rho	Age, Ma				D, %
	^{206}Pb	U		$^{207}Pb/^{235}U$	1σ	$^{206}Pb/^{238}U$	1σ		$^{207}Pb/^{235}U$	2σ	$^{206}Pb/^{238}U$	2σ	
1	97	2345	0.21	0.33172	1.5	0.04592	1.2	0.82	291	8	289	7	0.5
2	199	4627	0.15	0.34333	1.4	0.04768	1.2	0.88	300	7	300	7	–0.2
3	389	8952	0.15	0.34622	1.3	0.04808	1.2	0.90	302	7	303	7	–0.3
4	172	3743	0.18	0.37506	1.4	0.05098	1.2	0.87	323	8	321	8	0.9
5	150	3527	0.13	0.34019	1.4	0.04716	1.2	0.86	297	7	297	7	0.1
6	231	5252	0.17	0.35161	1.4	0.04867	1.2	0.88	306	7	306	7	–0.1
7	216	4992	0.19	0.34316	1.4	0.04796	1.2	0.87	300	7	302	7	–0.8
8	79	1700	0.24	0.37509	1.5	0.05105	1.2	0.83	323	8	321	8	0.8
9	50	1193	0.21	0.33204	1.7	0.04583	1.2	0.74	291	9	289	7	0.8
10	191	4368	0.11	0.34996	1.4	0.04826	1.2	0.89	305	7	304	7	0.3
11	151	3475	0.13	0.34416	1.4	0.04807	1.2	0.86	300	7	303	7	–0.8
12	204	4702	0.20	0.34767	1.4	0.04783	1.2	0.86	303	7	301	7	0.6
13	241	5583	0.19	0.34379	1.4	0.04765	1.2	0.87	300	7	300	7	0.0
14	83	1925	0.19	0.34401	1.5	0.04765	1.2	0.80	300	8	300	7	0.0
15	143	3067	0.30	0.37544	1.4	0.05129	1.2	0.86	324	8	322	8	0.4
16	188	4307	0.21	0.35035	1.4	0.04820	1.2	0.86	305	8	304	7	0.5
17	161	3488	0.21	0.37333	1.4	0.05109	1.2	0.85	322	8	321	8	0.3

Rho, correlation coefficient of errors of isotope ratios. D, discordance.

which have higher contents of Th (248–1314 ppm) and U (1193–8952 ppm) and low Th/U ratios (0.11–0.30) (Table 2). A broad range of U–Pb concordant ages is identified for 17 zircon grains with three generations evident, the U–Pb ages of which are 322.0 ± 3.7 (four grains), 301.6 ± 2.1 (11 grains), and 289.5 ± 4.9 Ma (two grains) (MSWD = 3.1, 0.17, and 0.98, respectively) (Fig. 4).

DISCUSSION

The range of U–Pb ages can be interpreted using a model of successive crystallization of different zircon generations in magmatic sources at various depths and their further capture upon differentiation and crystallization of new magma portions with the formation of new generations of this mineral in intrusive rocks [15]. According to this model, the "autocrysts" are zircon crystals that crystallize from the final and most differentiated portions of the magmatic melt; they are characterized by the youngest age. In contrast to them, the "antecrysts" are zircon crystals that crystallize in intermediate magmatic sources and chambers; they are characterized by a slightly older age, which is responsible for the dispersion of concordant U–Pb ages and corresponds to the successive evolution of a large long-lived source of partly crystallized magma (crystal mush magma) during its stagnation or transportation to deeper crustal levels. Finally, rare "xenocrysts" are zircon crystals that were trapped from older substrate rocks upon their partial or full melting.

The zircon crystals with a U–Pb age of ~322 and ~302 Ma, which probably indicate the presence of successively crystallizing magmatic source (or a series of sources) of granitoid magma at deeper levels, could thus be ascribed to "antecrysts" in the studied granodiorites–granites of the Sardara (Sarykty) pluton (Fig. 5a). Further, under conditions of intrachamber fractional differentiation and partial remelting, this deeper (peripheral) magmatic source could yield portions of more differentiated magma to higher levels, where it finally crystallized. Under these conditions, the "autocrysts" (zircon crystals with the youngest U–Pb age of ~289 Ma) could have formed in the studied rocks with older "antecrysts." The age of ~289 Ma corresponds to the Rb–Sr age of the studied rock (~286 Ma [9]), as well as the youngest U–Pb ages of other granitoid plutons in area of the Muruntau deposit (~293–288 Ma [7]).

The similarity of the U–Pb ages of two (youngest ~302 and ~289 Ma, respectively) zircon generations from granodiorites–granites of the Sardara (Sarykty) pluton with the concordant U–Pb ages previously measured for monzonite porphyries (303.3 ± 3.4 Ma)

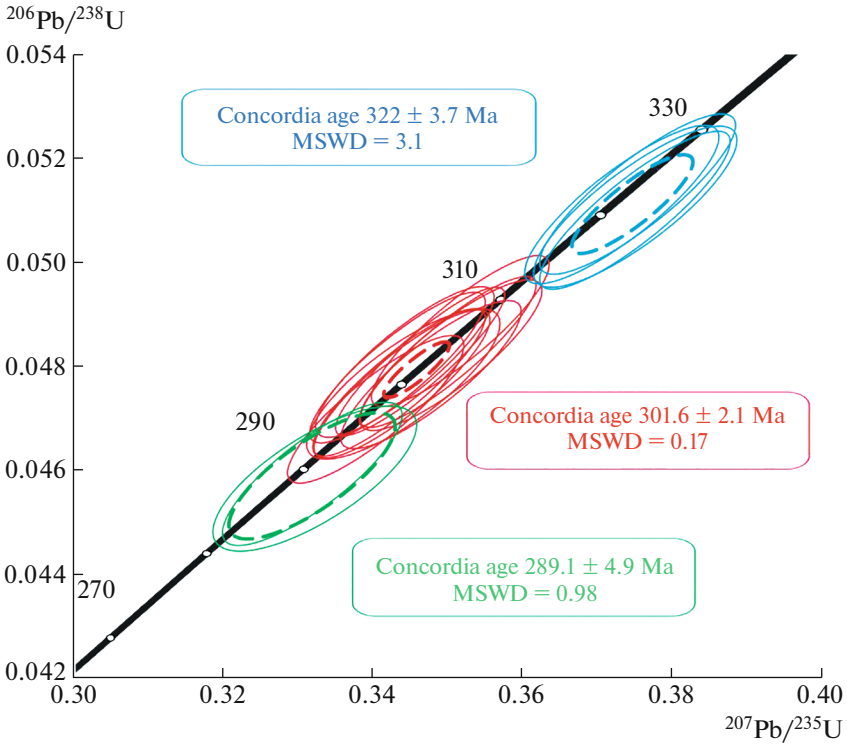

Fig. 4. Diagram with concordia for zircons from granodiorites–granites of the Sardara (Sarykty) pluton. Thin solid ellipses are the results of single analyses; the dotted ellipses correspond to concordant values in the group of analyses. The errors of single analyses and calculated concordant ages are given at the level of 2σ.

and Murun leucogranites–alaskites (291.9 ± 2.3 Ma) at the Muruntau deposit is noteworthy, although the reliability of the latter ages was doubtful because of the high U content of zircon, which was interpreted as indicating a postmagmatic (hydrothermal) origin of this mineral [7]. Small dikes and apophyses of granitoid rocks, which occur at this deposit, could thus be dike branchings at corresponding stages of evolution (progressive differentiation) of sources of granitoid magma of different depths, the larger intrusions of which include Sardara (Sarykty) and other plutons exposed at some distance from the deposit (Fig. 5a). Our U–Pb ages of intrusive rocks are thus slightly older than most isotopic age determinations of ore-bearing metasomatites and ore minerals of the Muruntau deposit (Fig. 5b), in particular, those for arsenopyrite of an early (?) gold-bearing assemblage (from 287.0 ± 2.5 to 295.4 ± 6.1 Ma according to the Re/Os method [16]), as well as those for scheelite (279 ± 18 Ma according to the Sm/Nd method [17]). A series of close isochrone Rb–Sr ages (272.6 ± 3.8 Ma, on average) was determined for quartz–K-feldspar metasomatites with arsenopyrite, scheelite, and native gold, which are crossed by a lamprophyric dike [9]. The isotopic ages of the most productive metasomatites of this deposit analyzed by different methods therefore lie in the range of 295–272 Ma, which, even taking into account the analytical error, coincides with the suggested latest stage of crystallization of granitoid rocks of the Sardara (Sarykty) pluton. This is also in accordance with overprinted metasomatites of most productive gold-bearing stage of the formation of the deposit on dikes of monzonite porphyries, which are probably the derivatives of slightly earlier (deeper?) sources of granitoid magma.

The graintoid dikes associated with the Sardara (Sarykty) pluton are crossed by late dikes of mafic porphyritic rocks. These dikes are younger, which is supported by their isotopic age. In particular, the isochrone Rb–Sr age of a dike of lamprophyres (kersantites) is 273.0 ± 3.0 Ma ($^{87}Sr/^{86}Sr$ = 0.7082) [9], whereas the K–Ar age of biotite from other dikes of monzodiorite porphyries and lamprophyres ranges from 247 ± 2 to 256 ± 7 Ma [18]. A similar $^{40}Ar–^{39}Ar$ age was identified for one of these dikes (251.9 ± 1.5 Ma [19]), which was however interpreted as the age of hydrothermal alteration of this dike. These changes could correspond to a later productive (gold–arsenopyrite–bismuth–telluride or gold-polymetallic) stage related to quartz–albite–sericite–chlorite metasomatites (Fig. 5b). The ages of these mostly albite metasomatites vary from 257 ± 13 and 230.2 ± 3.5 Ma (Rb–Sr method [8]) to 245 Ma ($^{40}Ar–^{39}Ar$ age of sericite [9]).

Our U–Pb ages of zircons from rocks of the Sardara (Sarykty) pluton, which are correlated with

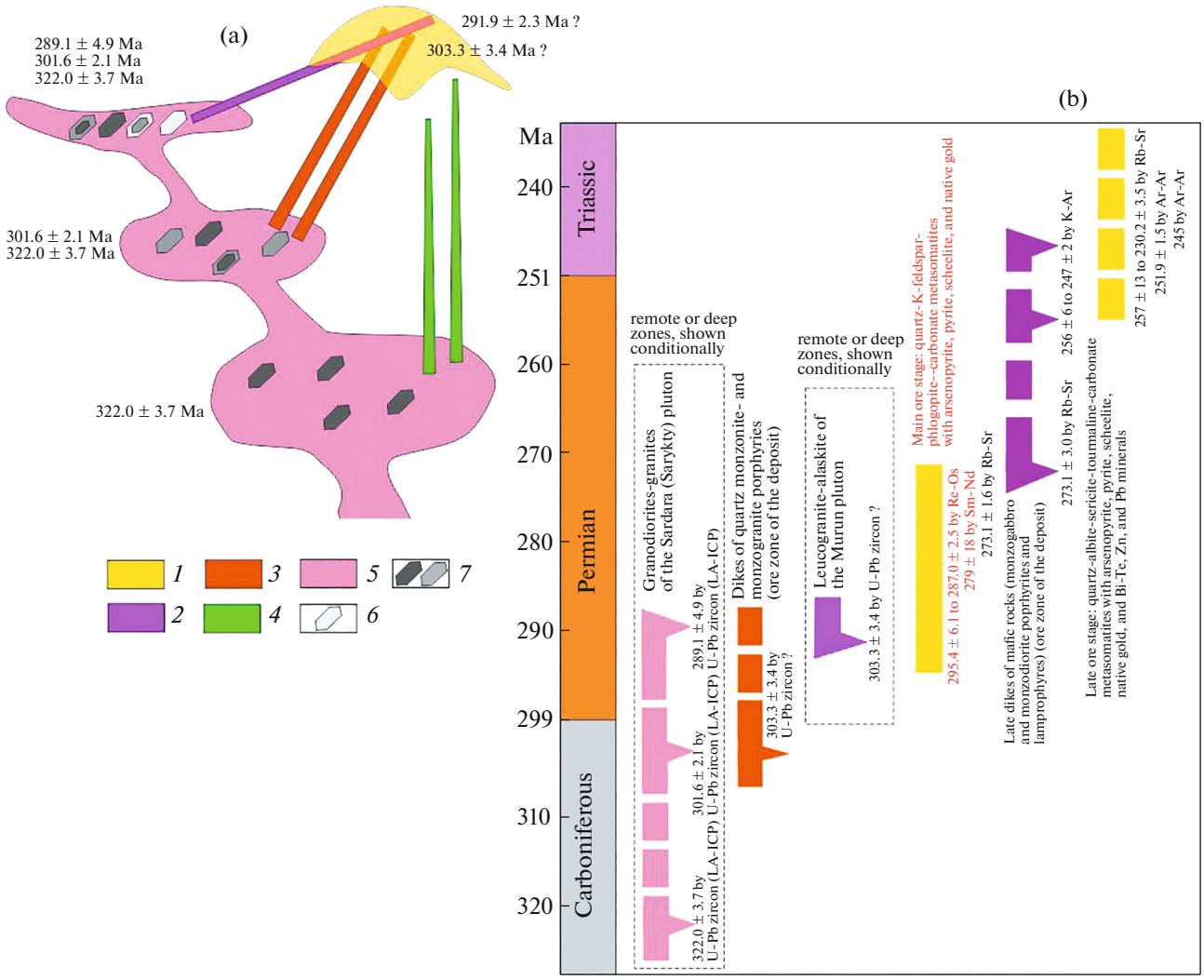

Fig. 5. Idealized model of distribution of different zircon crystal generations (including "antecrysts" and "autocrysts") in a series of successively formed magmatic sources at various depths (a) and the metallogenic scheme showing isotopic ages (Ma) of magmatic and hydrothermal stages of the formation of the Muruntau deposit (b). The isotopic ages of zircons from igneous rocks of the area of the Muruntau deposit are given from works [3, 7, 9, 16, 19]. (*1*) Mineralized zone of the Muruntau deposit; (*2*) apophyses and dikes of leucogranites-alaskites of the Murun pluton; (*3*) dikes of monzonite- and monzogranite porphyries; (*4*) possible dikes and stocks of less differentiated igneous rocks; (*5*) Sardara (Sarykty) pluton of granodiorites–granites; (*6*) zircon "autocrysts"; (*7*) older zircon "autocrysts" and "antecrysts" including relics in core parts of crystals.

the postgranite age of the main ore stage at the Muruntau deposit, are interesting for the revealing the position of potential ore-bearing magmatism in the geological evolution of the region. It is generally accepted that the transition from subduction (caused by convergence of the Kazakhstan and Tarim continents) to the postcollision stage in the Late Paleozoic occurred in Tien Shan at the very beginning of the Permian (Asselian Stage of the Early Permian ~295 Ma) [20]. With a typical short period after the subduction processes, the region was thus affected by Early Permian postcollision magmatism mostly dated at 295–280 Ma and characterized by intrusion of numerous granitoid plutons [5, 6]. The older U–Pb isotopic ages of zircon from granitoids of the Sardara (Sarykty) pluton (322 and 302 Ma) are therefore closer to the subduction stage, whereas the youngest zircons (289 Ma) correspond to the postcollision stage. Thus, the origination and initial evolution of magmatic sources in area of the Muruntau deposit occurred in subduction conditions, whereas the final differentiation and crystallization of granitoid magma finished at the postcollision stage. This postcollisional stage probably corresponds to the age of the formation of the main abundance of gold ores at the deposit. As a result, long evolution of the magmatic-ore system in transitional subduction–postcollision conditions is probably a distinctive feature of this giant deposit.

ACKNOWLEDGMENTS

We are grateful to A.V. Tyshkevich, Central Research Institute of Geological Prospecting for Base and Precious Metals, for selection and preparation of zircon samples.

FUNDING

This work was supported by state contracts of the Institute of Geology of Ore Deposits, Petrography, Mineralogy, and Geochemistry, Russian Academy of Sciences, Moscow (project no. 121041500220-0) and IGM SB RAS.

CONFLICT OF INTEREST

The authors declare that they have no conflicts of interest.

OPEN ACCESS

This article is licensed under a Creative Commons Attribution 4.0 International License, which permits use, sharing, adaptation, distribution and reproduction in any medium or format, as long as you give appropriate credit to the original author(s) and the source, provide a link to the Creative Commons license, and indicate if changes were made. The images or other third party material in this article are included in the article's Creative Commons license, unless indicated otherwise in a credit line to the material. If material is not included in the article's Creative Commons license and your intended use is not permitted by statutory regulation or exceeds the permitted use, you will need to obtain permission directly from the copyright holder. To view a copy of this license, visit http://creativecommons.org/licenses/by/4.0/.

REFERENCES

1. U. Kempe, T. Graupner, R. Seltmann, H. de Boorder, A. Dolgopolova, and M. Zeylmans van Emmichoven, Geosci. Front. **7**, 495–528 (2016).
2. Yu. S. Savchuk, E. E. Asadullin, A. V. Volkov, and V. V. Aristov, Geol. Ore Deposits **60** (5), 365–398 (2018).
3. R. Seltmann, R. Goldfarb, B. Zu, R. A. Creaser, A. Dolgopolova, and V. V. Shatov, SEG Spec. Publ. **23**, 497–521 (2020).
4. A. Yakubchuk, A. Cole, R. Seltmann, and V. Shatov, in *Integrated Methods for Discovery: Global Exploration in 21st Century,* Ed. by R. Goldfarb and R. Nielsen (Soc. Economic Geologists, 2020), Vol. 9, pp. 177–201.
5. A. Dolgopolova, R. Seltmann, D. Konopelko, Yu. S. Biske, V. Shatov, R. Armstrong, E. Belousova, R. Pankhurst, R. Koneev, and F. Divaev, Gondwana Res. **47**, 76–109 (2017).
6. R. Seltmann, D. Konopelko, G. Biske, F. Divaev, and S. Sergeev, J. Asian Earth Sci. **42**, 821–838 (2011).
7. U. Kempe, R. Seltmann, T. Graupne, N. Rodionov, S. A. Sergeev, D. I. Matukov, and A. A. Kremenetsky, Ore Geol. Rev. **65**, 308–326 (2015).
8. F. P. Bierlein and A. R. Wilde, Aust. J. Earth Sci. **57** (6), 839–854 (2010).
9. Y. A. Kostitsyn, Geochem. Int. **34**, 1009–1023 (1996).
10. W. L. Griffin, W. J. Powell, N. J. Pearson, and S. Y. O'Reilly, in *GLITTER: Data Reduction Software for Laser Ablation ICP-MS,* Ed. by P. Sylvester (Miner. Assoc. of Canada, 2008), Vol. 40, pp. 307–311.
11. J. Hiess, D. J. Condon, N. McLean, and S. R. Noble, Science **335**, 1610–1614 (2012).
12. J. Slama, J. Kosler, D. J. Condon, et al., Chem. Geol. **249** (1-2), 1–35 (2008).
13. K. R. Ludwig, *User's Manual for Isoplot3.00. A Geochronol. Toolkit for Microsoft Excel. Berkeley Geochronological Center Spec. Publ. No. 4* (Berkeley Geochronol. Center, Berkeley, CA, 2003).
14. L. P. Black, S. L. Kamo, C. M. Allen, et al., Chem. Geol. **205**, 115–140 (2004).
15. J. S. Miller, J. E. Matzel, C. F. Miller, S. D. Burgess, and R. B. Miller, J. Volcanol. Geotherm. Res. **167** (1/4), 282–299 (2007).
16. R. Morelli, R. A. Creaser, R. Seltmann, F. M. Stuart, D. Selby, and T. Graupner, Geology **35** (9), 795–798 (2007).
17. U. Kempe, B. V. Belyatsky, R. S. Krymsky, A. A. Kremenetsky, and P. A. Ivanov, Miner. Deposita **36**, 379–392 (2001).
18. A. D. Kanash, E. M. Golovin, and L. A. Yur'eva, *Tamdytau–South Nurata Region: Catalog of Geochronological Data (K–Ar Method)* (SAIGIMS, Tashkent, 1980), Vol. 1 [in Russian].
19. A. R. Wilde, T. Layer, T. Mernagh, and J. Foster, Econ. Geol. **96**, 633–644 (2001).
20. Yu. S. Biske, *The Southern Tien Shan: Paleozoic Structure and History* (St. Petersburg State Univ., St. Petersburg, 1996) [in Russian].

Translated by I. Melekestseva

Publisher's Note. Pleiades Publishing remains neutral with regard to jurisdictional claims in published maps and institutional affiliations.